

## Electronic supplementary information

# **A biomimetic all-inorganic photocatalyst for the artificial photosynthesis of hydrogen peroxide**

**Miwako Teranishi,<sup>1</sup> Shin-ichi Naya,<sup>1</sup> Yaozong Yan,<sup>2</sup> Tetsuro Soejima,<sup>2</sup>**

**Hisayoshi Kobayashi,<sup>3</sup> and Hiroaki Tada<sup>2\*</sup>**

<sup>1</sup> Environmental Research Laboratory, Kindai University, 3-4-1, Kowakae, Higashi-Osaka, Osaka 577-8502, Japan.

<sup>2</sup> Graduate School of Science and Engineering, Kindai University, 3-4-1, Kowakae, Higashi-Osaka, Osaka 577-8502, Japan.

<sup>3</sup> Emeritus Prof. Kyoto Institute of Technology, Matsugasaki, Sakyo-ku, Kyoto, 606-8585, Japan.

\* To whom correspondence should be addressed: TEL: +81-6-6721-2332, FAX: +81-6-6727-2024, E-mail: h-tada@apch.kindai.ac.jp

## Table of contents

1. Experimental Section .....	S3,4
2. Reference.....	S5
3. Supplementary Tables.....	S6,7
4. Supplementary Figures.....	S8-15

## Experimental Section

### Materials

SnO<sub>2</sub> NPs (mean particle size = 22-43 nm, specific surface area = 160 m<sup>2</sup> g<sup>-1</sup>) were purchased from FUJIFILM Wako Chem. Co. SnO<sub>2</sub> NPs (mean particle size ~100 nm) were purchased from Aldrich. Hydrogen tetrachloroaurate(III) tetrahydrate (HAuCl<sub>4</sub>·4H<sub>2</sub>O > 99%), sodium hydroxide (NaOH > 97.0%), antimony(III) chloride (SbCl<sub>3</sub> >98.0%), copper(II) sulfate pentahydrate (CuSO<sub>4</sub>·5H<sub>2</sub>O > 99.5%), 2,9-dimethyl-1,10-phenanthroline hemihydrate (C<sub>14</sub>H<sub>12</sub>N<sub>2</sub>·0.5H<sub>2</sub>O), phosphate buffer solution (pH 6.86), sodium perchlorate (NaClO<sub>4</sub> >96.0%) were purchased from Kanto Chemical Co. Fluorine-doped tin(IV) oxide film-coated glass (FTO, TEC7) was purchased from Aldrich. All chemicals were used as-received without further purification.

### Photocatalyst preparation.

Au NPs were loaded on commercially available SnO<sub>2</sub> NPs (FUJIFILM Wako Chem. Co., mean particle size = 22-43 nm, specific surface area = 160 m<sup>2</sup> g<sup>-1</sup>) by the deposition-precipitation method.<sup>1</sup> An aqueous solution of HAuCl<sub>4</sub> (4.86 mM, 50 mL) was neutralized to pH 6 by 1 M NaOH aq. SnO<sub>2</sub> NPs (5 g) were dispersed into the solution, and the suspension was stirred at 343 K for 1 h. The particles were collected by the centrifugation, and washed with distilled water. After drying, the resulting particles were calcined at 773 K for 4 h in the air to obtain Au/SnO<sub>2</sub>. SnO<sub>2</sub> or Au/SnO<sub>2</sub> (1 g) were dispersed into a methanol solution of SbCl<sub>3</sub> (0.2-50 mM, 50 mL), and placed in the dark at 293 K for 0.25 h. The resulting sample was washed with methanol, distilled water, and acetone, and dried in vacuo to obtain SnO<sub>2</sub>-Sb(III) or Au/SnO<sub>2</sub>-Sb(III). For comparison, Au NPs were loaded on SnO<sub>2</sub> NPs consisting of isolated particles (Aldrich, mean particle size ~100 nm) by the deposition-precipitation method using urea as a neutralizer.<sup>2</sup> SnO<sub>2</sub> NPs (0.8 g) and urea (1.17 g) were added into an aqueous solution of HAuCl<sub>4</sub> (4.86 mM, 40 mL), and stirred at 353 K for 12 h. The particles were collected by the centrifugation, and washed with distilled water. After drying, the resulting particles were calcined at 673 K for 1 h in the air to obtain Au/SnO<sub>2</sub>. Au/SnO<sub>2</sub> (0.2 g) were dispersed into a methanol solution of SbCl<sub>3</sub> (50 mM, 10 mL), and placed in the dark at 293 K for 0.25 h. The resulting sample was washed with methanol, distilled water, and acetone, and dried in vacuo to obtain Au/SnO<sub>2</sub>-Sb(III).

The Cl in the solution after the adsorption of SbCl<sub>3</sub> on SnO<sub>2</sub> NCs can exist as SbCl<sub>3</sub> and free Cl<sup>-</sup> ions. The mole numbers of Sb ( $n_{s,Sb}$ ) and Cl ( $n_{s,Cl}$ ) in the solutions were determined by ICP spectroscopy and ion chromatography, respectively. The subtraction of  $n_{s,Cl} - 3n_{s,Sb}$  yields the mole number of free Cl<sup>-</sup> ions in the solution ( $n_{s,Cl^-}$ ). Further, the number of Cl<sup>-</sup> ligands liberated by the adsorption ( $x$  in SbCl<sub>3-x</sub>) was calculated to be 1.6-2.0 by the ratio of  $n_{s,Cl^-}$  to the mole number of the Sb adsorbed on SnO<sub>2</sub> ( $n_{ad,Sb}$ ).

### Characterization

Sb loading amounts were quantized by using inductively coupled plasma spectroscopy (ICPE-9820, Shimadzu). Observations of a transmission electron microscopy (TEM) and high-resolution TEM were carried out by means of JEM-2100F (JEOL) operated with an applied voltage of 200 kV. The measurements of X-ray photoelectron spectroscopy (XPS) was carried out by using a Kratos Axis Nova X-ray photoelectron spectrometer with a monochromated Al K $\alpha$  X-ray source operated at 15 kV and 10 mA using C1s as the energy reference (284.6 eV). Diffuse reflectance UV-Vis-NIR

absorption spectra were collected by a UV-2600 spectrometer (Shimadzu) with integrating sphere unit (Shimadzu, ISR-2600Plus) at room temperature. The reflectance ( $R_\infty$ ) of the samples was recorded by using BaSO<sub>4</sub> as the reference. To obtain the relative absorption coefficient, the Kubelka-Munk function [ $F(R_\infty) = (1 - R_\infty)^2/2R_\infty$ ] was used. The photoluminescence (PL) spectra were collected by means of a JASCO FP-6000 spectrofluorometer with an excitation wavelength of 300 nm at 77 K.

### Adsorption isotherms of SbCl<sub>3</sub> on SnO<sub>2</sub>

SnO<sub>2</sub> NPs (50 mg) were dispersed into a methanol solution of SbCl<sub>3</sub> (0.2-50 mM, 50 mL), and placed in the dark at 293 K for 3 h. After the centrifugation, the supernatant was filtered by using PTFE membrane filter. The Sb amount of the solution was quantified by using inductively coupled plasma spectroscopy (ICPE-9820, Shimadzu).

### Photocatalytic H<sub>2</sub>O<sub>2</sub> production

Photocatalyst (10 mg) was dispersed into aerobic distilled water (10 mL) in an open-test tube, and stirred at 25 °C under illumination by LED lamp ( $\lambda_{\text{ex}} = 420 \pm 20$  nm,  $I = 8.1$  mW cm<sup>-2</sup>). After removing the particles, the concentration of H<sub>2</sub>O<sub>2</sub> was quantified by the colorimetric method using Cu(II) ion and 2,9-dimethyl-1,10-phenanthroline.<sup>3</sup> The external quantum efficiency ( $\phi_{\text{ex}}$ ) was calculated with assuming two-electron process as Eq. 1.

$$\phi_{\text{ex}} (\%) = \{2 \times (\text{number of H}_2\text{O}_2 \text{ molecules produced})/\text{number of incident photons}\} \times 100 \quad (1)$$

### Photoelectrochemical measurements

SnO<sub>2</sub> nanocrystalline film was formed on fluorine-doped tin oxide (FTO, Aldrich, TEC7). SnO<sub>2</sub> NPs were added to a solution of polyethylene glycol 20,000 (0.2 g), Triton X-100 (0.1 mL), and acetylacetone (1 drop) in distilled water (0.4 mL), and grinded to form the uniform paste. By the doctor blade technique, the paste was coated on FTO with 60  $\mu\text{m}$  thick, and the resulting sample was calcined at 773 K for 1 h to form mp-SnO<sub>2</sub>/FTO. The SnO<sub>2</sub>/FTO was immersed into a methanol solution of SbCl<sub>3</sub> (0.2-50 mM, 10 mL), and placed in the dark at 293 K for 3 h. The resulting electrode was washed with methanol, distilled water, and acetone, and dried in vacuo to obtain SnO<sub>2</sub>-Sb(III)/FTO. Photoelectrochemical measurements were performed by the standard three-electrochemical cell with the structure of SnO<sub>2</sub>-Sb(III)/FTO (working electrode) | 0.1 M NaClO<sub>4</sub> aqueous solution | Ag/AgCl (reference electrode) | glassy carbon (counter electrode). The working electrode was illuminated by monochromatic light using LED lamp.

### DFT simulations

DFT calculations with the periodic boundary conditions were carried out using a plane wave based program, CASTEP.<sup>4,5</sup> For the geometry optimization, the Perdew-Burke-Ernzerhof (PBE) functional<sup>6,7</sup> was used together with the ultrasoft-core potentials.<sup>8</sup> The basis set cutoff energy was set to 300 eV. For the present systems, the PBE functional afforded too narrow band gaps, and then the 1-point energy calculation was performed using the hybrid B3LYP functional,<sup>9</sup> the norm conserving core potentials<sup>10</sup> and the cutoff energy of 600 eV with the PBE optimized structures. The electron configurations of the atoms were O: 2s<sup>2</sup>2p<sup>4</sup>, Cl: 3s<sup>2</sup>3p<sup>5</sup>, Sn: 5s<sup>2</sup>5p<sup>2</sup>, and Sb: 5s<sup>2</sup>5p<sup>3</sup>. The slab mode was prepared by cleaving (110) face of bulk SnO<sub>2</sub>. Lattice parameters of the primitive cell were  $a = 3.186$  Å,  $b = 6.700$  Å,  $\alpha = \beta = \gamma = 90^\circ$ . The  $c$ -axis was taken in the direction of surface normal, and set to  $c = 19.286$  Å including the vacuum region. For calculation with adsorbates, the super cell with twice

the primitive cell was adopted ( $a = 6.373 \text{ \AA}$ ). For the atomic composition of slab models,  $(\text{SnO}_2)_{12}$  was adopted. Considering the hydrolysis reaction  $(\text{SnO}_2)_{12} + \text{H}_2\text{O} \rightarrow \text{HO}-(\text{SnO}_2)_{12}-\text{H}$ , and a successive reaction with  $\text{SbCl}_3$ ,  $\text{HO}-(\text{SnO}_2)_{12}-\text{H} + \text{SbCl}_3 \rightarrow [\text{O}-(\text{SnO}_2)_{12}]-\text{SbCl} + 2\text{HCl}$ , the composition of slab model was set to  $[\text{Sn}_{12}\text{O}_{25}]-\text{SbCl}$ . For a model of heavier concentration of  $\text{SbCl}$ ,  $[\text{Sn}_{12}\text{O}_{25}]-(\text{SbCl})_2$  model was also employed, where  $\text{SbCl}$  unit was bonded to the central and peripheral O atoms.

## References

1. S. Tsubota, M. Haruta, T. Kobayashi, A. Ueda and Y. Nakahara, *Preparation of catalysts V*, Elsevier, Amsterdam, 1991.
2. R. Zanella, S. Giorgio, C. R. Henry and C. Louis, *J. Phys. Chem. B*, 2002, **106**, 7634-7642.
3. K. Kosaka, H. Yamada, S. Matsui, S. Echigo and K. Shishida, *Environ. Sci. Technol.*, 1998, **32**, 3821-3824.
4. M. C. Payne, M. P. Teter, D. C. Allan, T. A. Arias, J. D. Joannopoulos, *Rev. Mod. Phys.*, 1992, **64**, 1045-1097.
5. V. Milman, B. Winkler, J. A. White, C. J. Pickard, M. C. Payne, E. V. Akhmatkaya, R. H. Nobes, *Int. J. Quantum Chem.*, 2000, **77**, 895-910.
6. P. Perdew, K. Burke and M. Ernzerhof, *Phys. Rev. Lett.*, 1996, **77**, 3865-3868.
7. P. Perdew, K. Burke, M. Ernzerhof, [Erratum to Document Cited in CA126:51093]. *Phys. Rev. Lett.*, 1997, **78**, 1396.
8. K. Laasonen, R. Car, C. Lee, D. Vanderbilt, *Phys. Rev. B*, 1991, **43**, 6796-6799.
9. A. D. Becke, *J. Chem. Phys.*, 1993, **98**, 5648-5652.
10. D. R. Hamann, M. Schluter and C. Chiang, *Phys. Rev. Lett.*, 1979, **43**, 1494-1497.

**Table S1.** Comparison of the activity of the metal oxide-based visible light photocatalysts for H<sub>2</sub>O<sub>2</sub> production.

Catalyst	Gas	Light wavelength (Intensity)	H <sub>2</sub> O <sub>2</sub> generation rate (mM g <sup>-1</sup> h <sup>-1</sup> )	External quantum yield (Φ <sub>ex</sub> )	Ref.
Au/SnO <sub>2</sub> -Sb(III)	Air	420 nm (8.1 mW cm <sup>-2</sup> )	6.1	1.1%	This work
Au/SnO <sub>2</sub> -Sb(III)	Air	Solar simulator (AM 1.5)	20.1		This work
Au/TiO <sub>2</sub>	Air	> 400 nm (AM 1.5 100 mWcm <sup>-2</sup> )	6.5×10 <sup>-2</sup>		11
Au/WO <sub>3</sub>	O <sub>2</sub>	420-500 nm (2.69 mW cm <sup>-2</sup> )	2.8×10 <sup>-2</sup>	---	12
Au/BiVO <sub>4</sub>	O <sub>2</sub>	420-500 nm (2.69 mW cm <sup>-2</sup> )	8.0×10 <sup>-2</sup>	0.25%	12
Graphene Oxide	Air	> 400 nm (Xe, 765 W)	0.63	---	13
N:Cu <sub>2</sub> O@CuO	Air	> 420 nm (Xe, 300 W)	0.84	---	14
Pt-PtO <sub>x</sub> /WO <sub>3</sub>	Air	> 420 nm (550 mW cm <sup>-2</sup> )	2.0	---	15
Au/WO <sub>3</sub>	Air	> 420 nm (4 mW cm <sup>-2</sup> )	1.6	---	16
Pd/Mo:BiVO <sub>4</sub> /CoO <sub>x</sub>	O <sub>2</sub>	Solar simulator (AM 1.5)	59.4	5.8%	17

11. N. Kaynan, B. A. Berke, O. Hazut and R. Yerushalmi, *J. Mater. Chem. A.*, 2014, **2**, 13822-13826.
12. H. Hirakawa, S. Shiota, Y. Shiraishi, H. Sakamoto, S. Ichikawa and T. Hirai, *ACS Catal.*, 2016, **6**, 4976-4982.
13. W.-C. Hou and Y.-S. Wang, *ACS Sustain. Chem. Eng.*, 2017, **5**, 2994-3001.
14. W. Zhang, X. Chen, X. Zhao, M. Yin, L. Feng and H. Wang, *Appl. Surf. Sci.*, 2020, **527**, 146908/1-9.
15. W. Xie, Z. Huang, R. Wang, C. Wen and Y. Zhou, *J. Mater. Sci.*, 2020, **55**, 11829-11840.
16. Y. Wang, Y. Wang, J. Zhao, M. Chen, X. Huang and Y. Xu, *Appl. Catal. B*, 2021, **284**, 119691/1-11.
17. T. Liu, Z. Pan, J. M. M. Vequizo, K. Kato, B. Wu, A. Yamakata, K. Katayama, B. Chen, C. Chu, K. and Domen, *Nat. Commun.*, 2022, **13**, 1034/1-8.

**Table S2.** Comparison for H<sub>2</sub>O<sub>2</sub> adsorption amount on metal oxides.

Metal oxides	H <sub>2</sub> O <sub>2</sub> <sub>ad</sub> ( $\mu\text{mol g}^{-1}$ )	H <sub>2</sub> O <sub>2</sub> <sub>ad</sub> ( $\mu\text{mol m}^{-2}$ )
SnO <sub>2</sub>	0.437	0.004
SnO <sub>2</sub> -Sb(III) $\Gamma_{\text{ad}} = 0.18$	2.08	0.021
SnO <sub>2</sub> -Sb(III) $\Gamma_{\text{ad}} = 0.56$	3.88	0.039
Anatase TiO <sub>2</sub>	7.01	0.070
Rutile TiO <sub>2</sub>	7.70	0.077
SrTiO <sub>3</sub>	8.60	0.434
BiVO <sub>4</sub>	1.80	1.295
Bi <sub>2</sub> O <sub>3</sub>	9.60	2.240
WO <sub>3</sub>	2.10	0.251
ZrO <sub>2</sub>	9.60	0.096

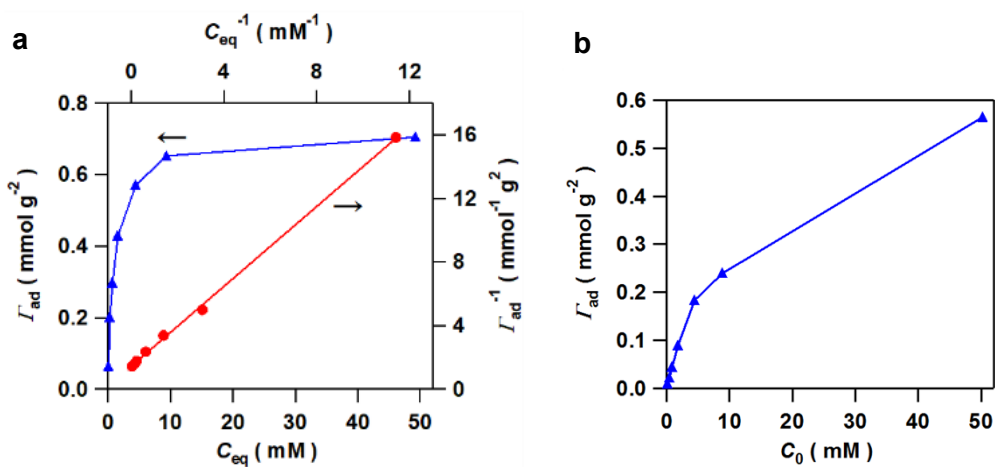


**Fig. S1.** (a) Adsorption isotherm of SbCl<sub>3</sub> on SnO<sub>2</sub> at 293 K (blue curve), and the Langmuir plot (red straight line). SbCl<sub>3</sub> was adsorbed on SnO<sub>2</sub> NCs from the methanol solution for 3 h at 293 K to achieve adsorption equilibrium. (b) Adsorption amounts of SbCl<sub>3</sub> on SnO<sub>2</sub> NCs from the methanol solution at 293 K vs. initial concentration of SbCl<sub>3</sub> ( $C_0$ ). SbCl<sub>3</sub> was adsorbed on SnO<sub>2</sub> NCs from the methanol solution for 15 min at 293 K.

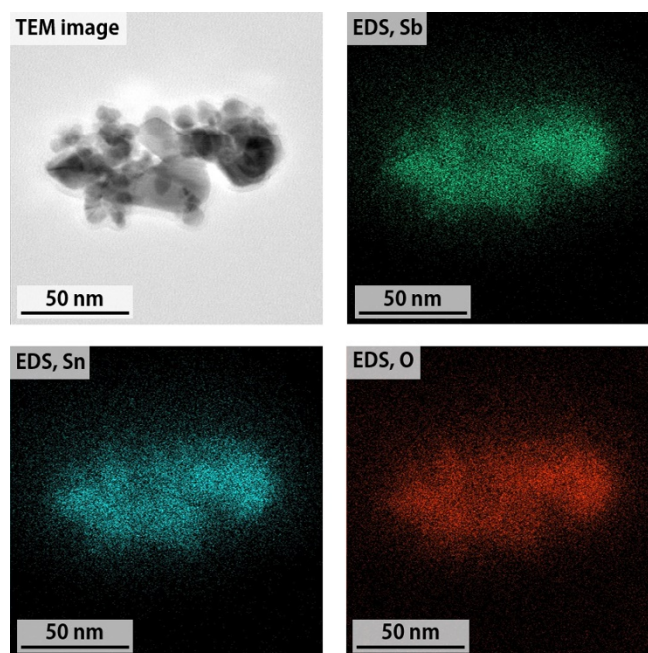


**Fig. S2.** TEM-EDS mapping of SnO<sub>2</sub>-Sb(III) prepared at C<sub>0</sub> = 50 mM.

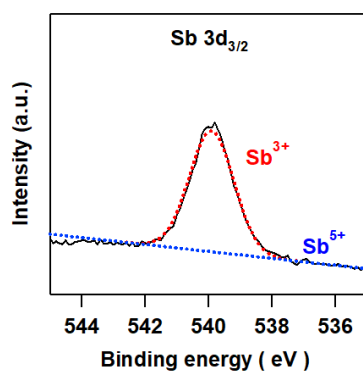


**Fig. S3.** Deconvoluted Sb 3d<sub>3/2</sub>-XP spectrum for SnO<sub>2</sub>-Sb(III) with  $\Gamma_{\text{ad}} = 0.56 \text{ mmol g}^{-1}$ .

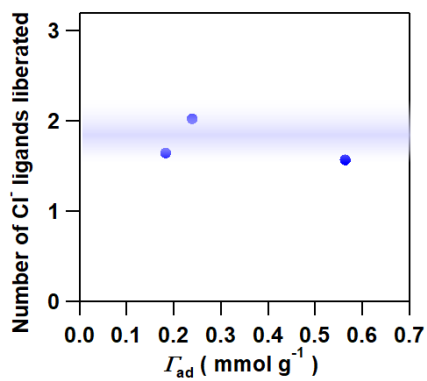


**Fig. S4.** Number of Cl<sup>-</sup> ligands liberated by the adsorption.

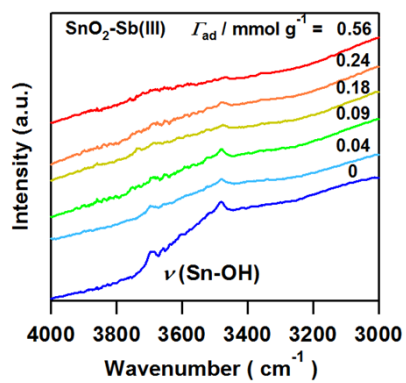


**Fig. S5.** DRIFT spectra of SnO<sub>2</sub>-Sb(III) with varying  $\Gamma_{ad}$ .

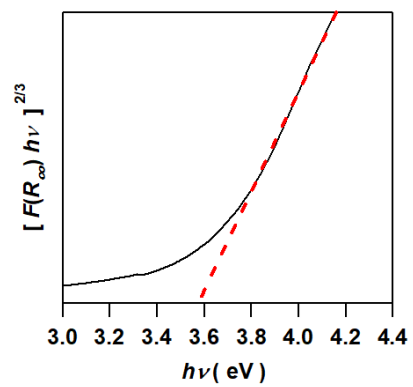


**Fig. S6.** Tauc plots for the absorption spectrum of unmodified SnO<sub>2</sub>.

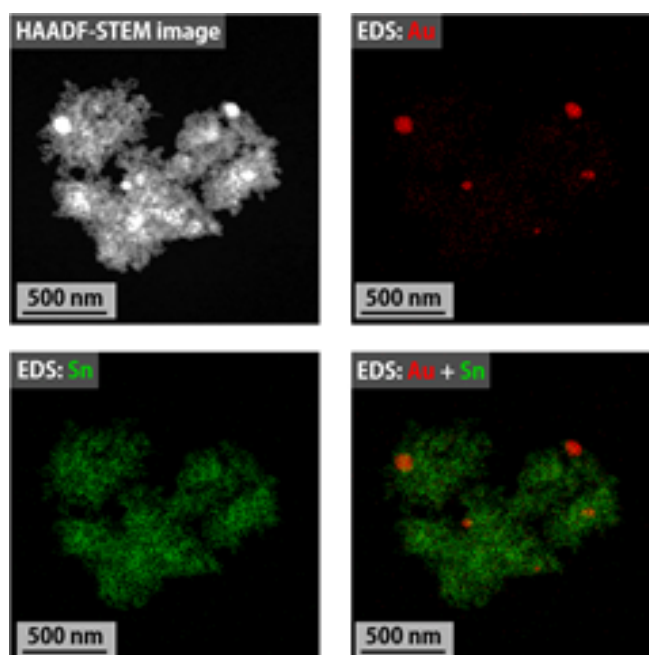


**Fig. S7.** TEM-EDS mapping of Au@SnO<sub>2</sub>.

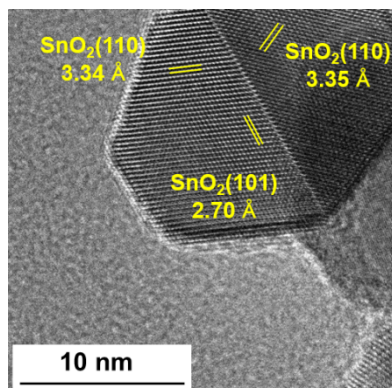


**Fig. S8.** Homoepitaxial junction between SnO<sub>2</sub> NCs with an orientation of (101)<sub>SnO2</sub>//(101)<sub>SnO2</sub>.

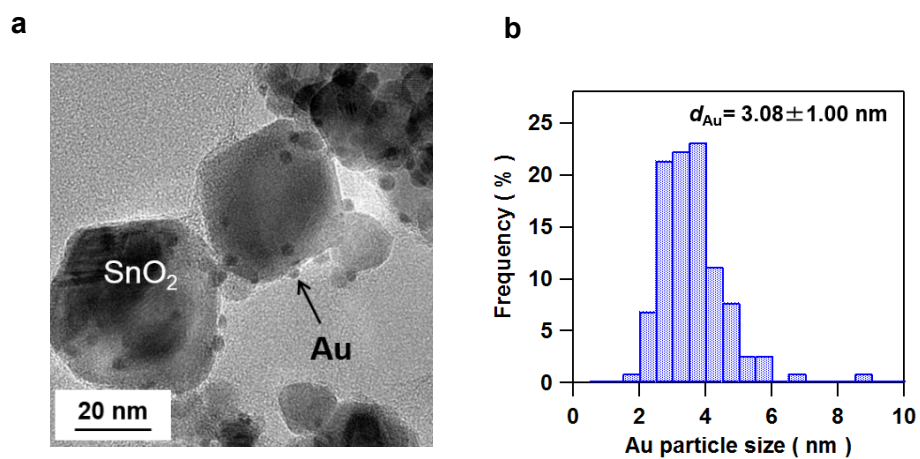


**Fig. S9.** TEM image (a) and Au particle size distribution (b) of Au/SnO<sub>2</sub>-Sb(III) prepared at C<sub>0</sub> = 50 mM.

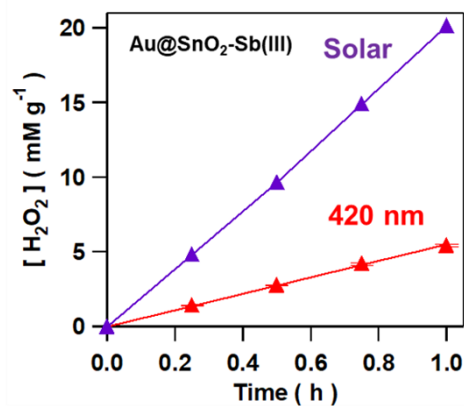


**Fig. S10.** Comparison of the photocatalytic activity of Au@SnO<sub>2</sub>-Sb(III) ( $\Gamma_{\text{ad}} = 0.18$  mmol g<sup>-1</sup>) for H<sub>2</sub>O<sub>2</sub> generation from water and O<sub>2</sub> under visible-light irradiation ( $\lambda_{\text{ex}} = 420$  nm) and simulated sunlight (AM-1.5, one sun) at 298 K.

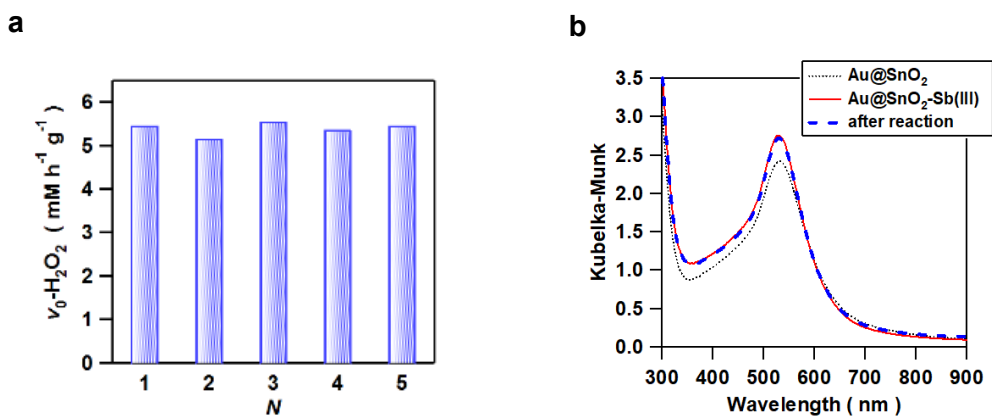


**Fig. S11.** (a) Stability test of the Au/SnO<sub>2</sub>-Sb(III) ( $\Gamma_{\text{ad}} = 0.56$ ) photocatalyst for H<sub>2</sub>O<sub>2</sub> generation. (b) Absorption spectra of Au@SnO<sub>2</sub>-Sb(III) before and after 5 times repeated reaction.

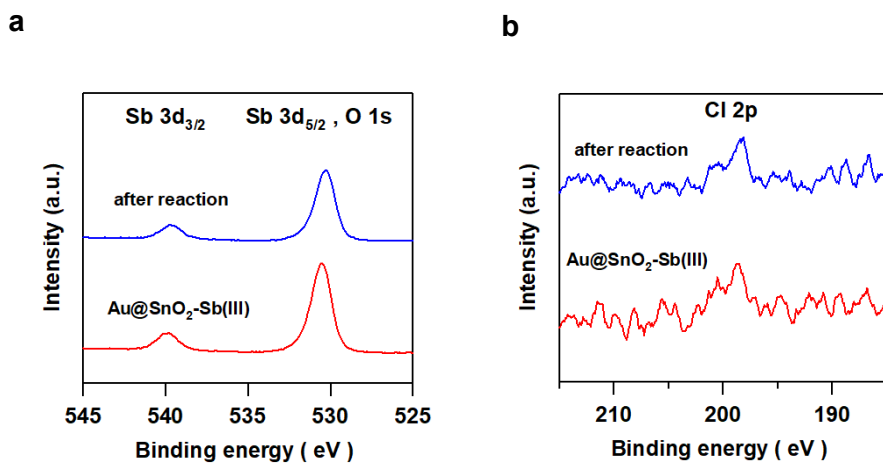


**Fig. S12.** Sb3d (a) and Cl2p-XP (b) spectra of Au@SnO<sub>2</sub>-Sb(III) before and after the repeated reactions.

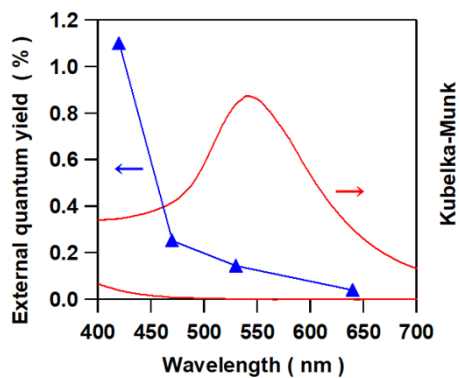


**Fig. S13.** Action spectrum of the external quantum yield for the reaction in the Au@SnO<sub>2</sub>-Sb(III) system.

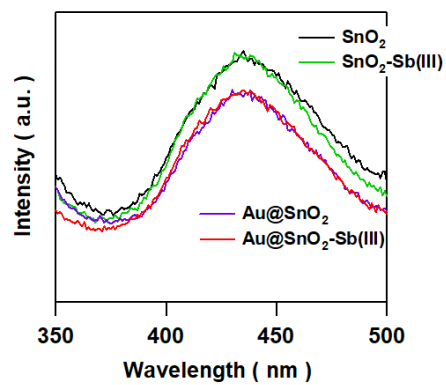


**Fig. S14.** Photoluminescence spectra of SnO<sub>2</sub>, Au@SnO<sub>2</sub>, SnO<sub>2</sub>-Sb(III), and Au@SnO<sub>2</sub>-Sb(III) were measured with excitation wavelength of 300 nm at 77 K.